Case Studies in Thermal Engineering 28 (2021) 101379

Contents lists available at ScienceDirect

Case Studies in Thermal Engineering

journal homepage: www.elsevier.com/locate/csite

Use of thermoelectric generators to harvest energy from motor vehicle brake discs

Adama Coulibaly [a], Nadjet Zioui [a,*], Said Bentouba [b], Sousso Kelouwani [a], Mahmoud Bourouis [c]

[a] Université du Québec à Trois-Rivières, 3351 Boulevard des Forges, Trois-Rivières, QC G8Z 4M3, Canada
[b] Faculty of Engineering and Science, Western Norway University of Applied Sciences, Bergen, 5063, Norway
[c] Universitat Rovira i Virgili, Department of Mechanical Engineering, Av. Països Catalans No. 26, 43007 Tarragona, Spain

HIGHLIGHTS

- A novel approach that uses thermoelectric generators to recover energy from automotive braking systems is applied.
- Finite element method is applied to thermal analysis of energy generation by braking under three climate scenarios.
- Most of the on-board instrumentation of an electric vehicle could be powered by recovering energy associated with braking.

ARTICLE INFO

Keywords:
Energy harvesting
Thermoelectric generator (TEG)
Thermal analysis
Finite element method (FEM)
Disc-pads friction

ABSTRACT

The challenge of reducing vehicle energy consumption and greenhouse gas emissions has become a major orientation of automotive industry research throughout the world. Improving and optimizing power consumption by electric vehicles is of special concern. A novel use of thermoelectric generators in vehicle braking is presented. Thermal analysis of brake pads and discs using finite elements was applied to evaluate the energy potentially available in the form of heat produced by the friction involved in braking. We present stimulations of disc heating during and after braking at three ambient temperatures and reflect on the possibilities of energy recovery in warm as well as cold climates. The results show that although the yield of electrical energy from typical thermoelectric generators is about 0.3% of the total thermal energy associated with braking, at least 4 W can be made available, enough to power on-board instrumentation and vehicle devices and thereby improve the energy efficiency of motor vehicles.

1. Introduction

Battery-powered electric vehicles that are being proposed to replace fossil-fuel-powered vehicles face the challenge of maximizing energy efficiency. So far, the most widely studied approach to achieving this has been energy consumption management, which solicits driver behaviour and experience.

Energy harvesting refers to processes by which useable energy is derived from ambient sources external to energy-using devices. Research and development in this area have become effervescent in recent years. Studies have shown that energy consumption by on-

* Corresponding author.
E-mail addresses: Adama.Coulibaly@uqtr.ca (A. Coulibaly), nadjet.zioui@uqtr.ca (N. Zioui), Said.Bentouba@hvl.no (S. Bentouba), Sousso.Kelouwani@uqtr.ca (S. Kelouwani), mahmoud.bourouis@urv.cat (M. Bourouis).

https://doi.org/10.1016/j.csite.2021.101379
Received 26 February 2021; Received in revised form 10 August 2021; Accepted 22 August 2021
Available online 26 August 2021

Nomenclature

TEG	Thermoelectric Generator
FEM	Finite Element Method
EH	Energy Harvesting
V	Vehicle speed (m/s)
L	Brake disk diameter (m)
$v0$	Initial speed (m/s)
vf	Final speed (m/s)
xf	Final position (m)
$x0$	Initial position (m)
tb	Braking time (s)
v	Speed (m/s)
g	Gravitational force (N/kg)
Ec	Kinetic energy (J)
m	Vehicle mass (kg)
ET	Energy total loss
P	Braking Power
$qtotal$	Total dissipated heat

Greek symbols

ρ	Air density ($kg/m3$)
μ	Dynamic viscosity of the air ($kg/m \cdot s$)
α	Thermal diffusivity of the air ($m2/s$)
a	Acceleration ($m/s2$)
$\lambda disc$	Thermal conductivities of the disc ($W/m.K$)
λpad	Thermal conductivities of the pad ($W/m.K$)

board instrumentation and smart processes represents about 14% of the total energy needs of an electric vehicle, sensors alone consuming about 9% [1]. New energy sources would have a considerable effect on the long-term energy efficiency and autonomy of such vehicles. Much published research in this area has focused on analysis of the thermal energy that accumulates in disc pads during braking and on disc design to optimize energy evacuation. Moreover, several studies of heat recovery in the form of electrical energy to improve the efficiency of machines in industrial settings have been published. This conversion of heat to electricity is possible using thermoelectric generators, which exploit temperature differentials across module faces by the Seebeck effect. Finite element methods of thermal analysis of solid brake discs are the subject of numerous articles. Heat transfer in full discs and ventilated discs [2,3,6] and temperature variations during and after braking have been compared [8]. Thermal behaviour has been investigated using the parabolic heat conduction equation [4] and FEM analysis of disc brakes has been implemented using SolidWorks software [5]. Iron and composite materials have been compared in transient analysis of heat in full and ventilated brake discs subjected to repeated braking cycles [9]. Brake disc structural changes and temperatures reached during repeated breaking have also been studied [10,12,13]. Dependency of the convective heat transfer coefficient on angular velocity has been shown [11]. Zabek et al. [14] reviewed solid-state generators for waste heat recovery and thermal energy harvesting have been reviewed. Thermoelectric, thermionic, pyroelectric and thermomagnetic generators and converters can be used to harvest thermal energy from temperature gradients or transient changes of temperature. These studies all suggest significant potential for thermal energy recovery when temperature differentials reach hundreds of degrees Celsius. Rotor designs have been compared by transient thermal analysis of vented disc rotors [15]. Champier [16] presented a review on thermoelectric generation applications covering electricity generation in extreme environments, waste heat recovery in transport and industry, domestic production in developing and developed countries, micro-generation for sensors and microelectronics and solar thermoelectric generators. A comparison of segmented and conventional thermoelectric generators in terms of response to variables such as heat source temperature, cold source temperature, heat transfer coefficient and thermocouple cross-sectional area has shown that the maximal power output and conversion efficiency of segmented generators are significantly higher when diesel engine exhaust is used as the heat source and coolant as the cold source [17]. All aspects of thermal energy harvesting systems development are the subject of a comprehensive thesis [18]. Harvestable energy dissipated by the human body has been measured using thermoelectric generators worn on arms and legs during activities such as walking, jogging, cycling and resting in a sitting position [19]. The power generated under these conditions ranges from 5 to 50 μW. At the other extreme, thermoelectric generators have been used to harvest industrial waste heat from sources such as boilers, turbines, smelters and furnaces [20]. In a recent work, thermoelectric generators have been considered to harvest heat energy from roadway pavements [21]. Finite Element (FE) analysis was performed and laboratory prototypes tested underlining promising potential of 5.4 kWh/day for an installation covering 1 km of roadway. Despite their low efficiency, thermoelectric generators could be used to provide electricity in quantities sufficient to power vehicle instruments and on-board computers, given that thermocouples operate from −270 °C to 1370 °C with output voltages ranging from −6.5 mV to 55 mV at hot-side temperatures ranging from 35 °C to 320 °C [22–28]. Recycling energy currently wasted in brake

pad discs represents a novel approach to improving the energy efficiency of electric vehicles. Finite element thermal analysis of brake disc pad friction allows a comparative study of several temperature scenarios, thus informing about the thermal energy available for harvesting while characterizing the influence of the ambient temperature on thermal energy and hence energy conversion performance in both warm and cold climates.

Since braking results from friction between the discs and the pads, temperatures on the disc surface can reach a few hundreds of degrees Celsius when a vehicle decelerates. In the present study, we present the concept of harvesting thermal energy that accumulates in disc pads during braking, in a useable form, namely electricity, to improve the energy autonomy of electric vehicles.

2. Materials and methods

The concept presented in this paper includes a thermal energy source and a transducer that allows the conversion of thermal energy into electrical energy. All motorized vehicle braking systems generate heat when solicited, due to the friction between the pads and the rotating disc. The heat flow depends on several parameters including the disc and pad materials (the coefficient of friction), the disc rotation speed and the pressure exerted by the pads. Better knowledge of the thermal behaviour of brakes will lead to a better understanding of the energy available and hence the potential for thermoelectric conversion and generation of electrical energy.

2.1. Brake disc

The brake disc rotates while the vehicle is moving and allows energy dissipation during braking. The disc alone absorbs nearly 90% of the heat flow from the friction developed between the pads and the disc when these parts are forced into contact under the pressure exerted by the calliper piston. Given the wide variety of motorized vehicles, many types of brake discs have been developed. Most are either full discs or slotted or drilled discs. Many different materials are used, but the most common are grey cast iron or steel. Some very expensive brake discs are made of carbon-ceramic alloys.

2.2. Brake pads

Brake pads come in a wide variety of geometries that are supposedly optimized for specific vehicles. Pads comprise two main elements, namely a lining and a support plate. The latter is made of galvanized steel and allows mounting around the disc via the calliper. The lining is in contact with the disc during braking and absorbs 10% of the heat generated by friction. Linings are made usually of ceramics, semi-ceramics and ferrous materials.

2.3. Thermoelectric generators

Thermoelectric devices convert heat to electrical energy thanks to the Seebeck effect and the Peltier effect. The transducers that make this conversion possible are thermocouples, the principle of which is illustrated in Fig. 1.

When two dissimilar materials (metals 1 and 2) are connected through a cold junction that is heated (the sensing junction), a voltage arises in the materials. This principle has been used widely to measure temperature, since the voltage generated has a fixed relationship to temperature, depending on the types of the materials. This is known as the Seebeck effect.

Advanced materials with enhanced electrical response to heat have been developed for thermal energy harvesting. Thermoelectric generators may be regarded as networks of connected thermocouples optimized for electrical energy generation [10]. Fig. 2 a and Fig. 2 b illustrate schematically a typical thermoelectric generator architecture and its equivalent electrical circuit, respectively.

Some commercially available thermoelectric generators can produce about 6.8 W at 2.0 V with a 3.4 A load at 180 °C, and 14 W at 4.2V and 3.4 A load at 300 °C, based on matched load outputs [23–25]. Recovery of thermal energy from brake discs involves temperatures of 300 °C–400 °C, depending on speed and the braking pressure applied. Some thermoelectric generators are rated for operating temperatures as low as 35 °C [23,25,30,31]. Thermal analysis of braking is important in order to determine the generator location that is optimal for energy harvesting.

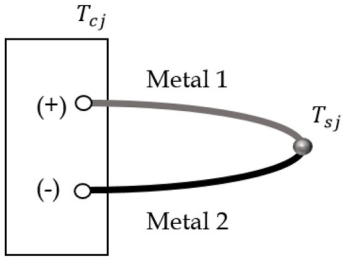

Fig. 1. Seebeck (thermocouple) effect used in thermal-electrical energy conversion (Adapted from Ref. [23]).

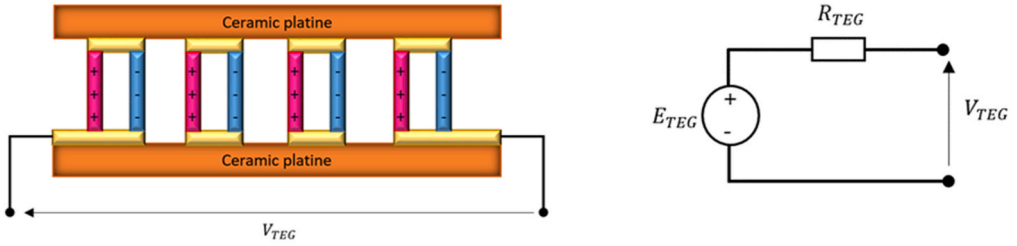

a) Typical TEG architecture.

b) Basic TEG equivalent electrical circuit

Fig. 2. Thermoelectric generator typical architecture and equivalent electrical circuit: a) Typical TEG architecture. b) Basic TEG equivalent electrical circuit. (Images adapted from Refs. [19,20,29]).
a) Typical TEG architecture.
b) Basic TEG equivalent electrical circuit

2.4. The finite element analysis method

SolidWorks 2019 was used to simulate thermal flow distribution in the brake disc and pads, and the finite elements method was used to analyse the model. A very common vehicle in North American was chosen, namely the Honda Civic [32]. The 2018 model has a 1.5 VTEC, a mass of 1425 kg, 406.4 mm wheel diameter, 4,994 mm^2 pad surface (Ap) with power/mass ratio of 94 W/kg [33]. Table 1 summarizes the mechanical characteristics of the brake disc and pad materials, and the dimensions are shown in Table 2 and Table 3.

Two types of discs were considered, with the same diameter but different thicknesses and profile shapes. The same pads were used in both simulations. The transient state braking time was set at 3.4 s with a 0.1 sampling rate. 3D models of the parts were developed using SolidWorks. Fig. 3 a. shows the brake disc-pad assemblies for the full disc case and Fig. 3 b. illustrates the ventilated disc case, both with the applied mesh. The following limit conditions were applied: heat flux to both sides of the disc, 896,519 W/m2; to pad linings, 996,13.2 W/m2 with an applied convection coefficient of 70 W/m2·K.

Because of the complexity of prediction of the materials properties considering evolutionary temperatures, some hypotheses have been formulated in order to perform the simulation. Among these hypotheses, the material properties have been considered constant.

2.5. Computations and hypotheses

Modelling the thermal behaviour of disc brakes is not a simple procedure, in particular during the transient phase [6]. In order to define the limit conditions for the simulation, computations must be used to estimate braking duration and power as well as heat flow. Based on published data, our computations incorporated the assumption that at an initial speed of 60 km/h or 16.67 m/s, the stop distance on a flat track was 28 m. We also assumed that the front brakes provided 60% of the braking and the back brakes 40% [34].

Computation of the coefficient of convection was based on tables of atmospheric pressure versus temperature and on interpolation [38]. This made it possible to determine the contribution of air properties. The Reynolds number (Re) was estimated as follows [39]:

$$R_e = \frac{\rho * V * L}{\mu} \tag{1}$$

ρ air density (kg/m^3)
V vehicle speed (m/s^2)
L brake disk diameter (m)
μ dynamic viscosity of the air ($kg/m \cdot s$)
The Prandtl number (Pr) at 25 °C is calculated as follows:

Table 1
Mechanical characteristics of the brake system parts [33,34].

	Discs (grey font)	Trim (ceramic)	Trim support (sheet steel)
Young's modulus E (MPa)	66,178.1	1000	205,000
Density ρ (kg/m^3)	7200	1400	7858
Poisson coefficient ν	0.27	0.25	0.29
Coefficient of friction μ	0.2	0.2	0.2
Coefficient of thermal expansion (/K)	1.2 10^{-5}	1.10^{-5}	1.2 10^{-5}
Thermal conductivity (W/m·K)	510	1000	420
Specific heat (J/kg·K)	66,178.1	1000	205,000

Table 2
Brake disc dimensions [35,36].

Parameter	Value
Height	47.2 mm
Centring diameter	64.1 mm
Disc thickness	25 mm–22.4 mm (max, min)
Diameter	280 mm
Internal diameter	142.2 mm
Drill circle	114.3 mm
Number of holes	5
Height	47.2 mm

Table 3
Brake pad dimensions [37].

Parameter	Value
Thickness	17.3 mm
Height	57 mm
Width	142 mm//156

Fig. 3. Mesh views of disc-pad automobile assemblies: a) Full disc and pad, b) Ventilated disc and pad.
(a) Full disc and pad
(b) Ventilated disc and pad

$$P_r = \frac{\nu}{\alpha} \tag{2}$$

ν kinematic viscosity of the air (m^2/s)
α thermal diffusivity of the air (m^2/s)
The Nusselt number (Nu) is computed using the following relationship [39]:

$$N_u = \frac{hL}{k} \tag{3}$$

The coefficient of convection is then estimated as follows:

$$h = \frac{N_u * k}{L} \tag{4}$$

k the thermal conductivity of air ($W/m \cdot K$)
h the convection coefficient ($W/m^2 \cdot K$)
Considering air 0 °C and −20 °C, the following results are obtained for the convection coefficient h:
At 0 °C, $h = 72 W/m^2 \cdot K$

At -20 °C, $h = 77.4 W/m^2 \cdot K$

The vehicle deceleration is estimated as follows [36]:

$$a = \frac{v_f^2 - v_0^2}{2(x_f - x_0)} \tag{5}$$

a acceleration (m/s^2)
v_f final speed (m/s)
v_0 initial speed (m/s)
x_f final position (m)
x_0 initial position (m)

Deceleration is equivalent to $0.5 \times g$.

The braking duration is estimated as follows:

$$t_b = \frac{v}{a * g} \tag{6}$$

t_b braking time (s)
v speed (m/s^2)
g gravitational force (N/kg)

Kinetic energy losses are computed as follows:

$$E_c = \frac{1}{2} m v^2 \tag{7}$$

E_c kinetic energy (J)
m vehicle mass (kg)

The total energy loss E_T takes into consideration rotational energy, which is estimated at 3% of the kinetic energy [36].

$$E_T = 1.03 * \ E_c = 203,936 J \tag{8}$$

And the total braking power P is estimated as follows:

$$P = \frac{E_T}{t_b} \tag{9}$$

For simulation purposes, we considered only 30% of the total power computed using equation (9). This is due to the braking efficiency distribution of 60% and 40% between the front and back wheels and sharing 60% between the two front braking discs. Consequently, the amount of power considered for the simulation was 17,994.36 W.

The total dissipated heat flow q_{total} (W/m^2) between the disc and pad is computed as follows:

$$q_{total} = 2 * \frac{4P}{\pi(D^2 - d^2)} \tag{10}$$

Which is the sum of the heat flow distributions inside the disc, q_{disc}, and in the pad, q_{pad}. Also:

$$\alpha = \frac{q_{pad}}{q_{total}} \tag{11}$$

$$q_{disc} = (1 - \alpha) q_{total} \tag{12}$$

$$\alpha = \frac{\lambda_{pad}}{\lambda_{pad} + \lambda_{disc}} \tag{13}$$

$$q_{disc} = (1 - \alpha) q_{total} \tag{14}$$

Where λ_{disc} and λ_{pad} are the thermal conductivities of the disc and pad, respectively, in $(W/m.K)$.

Table 4
FEM simulation parameters.

	Element type	Jacobian point	Mesher	Amount of elements	Nodes	Min element size (mm)	Max element size (mm)
Full disc and pad	Volume	4 points	Curvature-Based	48403	81578	2.12	10,59
Vented disc and pad	Volume	4 points	Curvature-Based	88151	145290	2,22	11,12

$$q_{pad} = \alpha * q_{total} \tag{15}$$

The 3D elements for thermal analysis that have been used during the modelling are presented in Table 4.

Table 5 summarizes the several computed parameters and variables that have been used to perform the FEM simulation.

In this study about the dissipated energy during the braking process using kinematic friction triggered by the contact of the disc and pads, the Finite Elements Method has been used in order to simulate this dynamical interaction. The simulation time was considered as 3.4 s and corresponds to the braking time with an increment time of 0.1 s. Moreover, the following has been considered:

- The materials properties are homogenous and stable with temperature.
- The pressure of contact between the disc and pads are evenly distributed.
- The coefficient of friction between the disc and pads is constant $\mu = 0.2$ for computations simplifications [2].
- The boundary conditions for the convection are set on all the boundaries.
- The convection is applied on the whole disc and lateral surfaces of the pads.
- The heat flow generated by friction is applied on the disc and the pads according to the results obtained in equations (7) and (8).

2.6. Thermal to electrical energy conversion

For experimental measurement of the electrical energy obtainable from the brakes, a thermoelectric generator suitable for braking temperatures in the 100–300 °C range was selected. The equivalent electrical circuit shown in Fig. 2 b. was presumed to represent the behaviour of the device. The generator was thus considered to be a temperature-gradient-dependent voltage source. Data are routinely obtained using open-circuit experiments and the "load-matched output power" technique [25]. A generator rated at 320 °C operating under load conditions at 25 °C gives the data shown in Fig. 4.

It is clear in Fig. 4 a. that the open-circuit output voltage is proportional to the hot-side temperature of the generator, which is expected since the device is in contact with the hotter face of the disc when the vehicle stops.

In both Fig. 4a and 4 b., the cool side of the device is presumed to be at an ambient temperature of about 25 °C. It should be noted that at higher cool-side temperatures, the output voltage can drop by about 1 V per 25 °C increment. Fig. 4 b. shows that the resistance of the device increases somewhat with the hot-side temperature, rising from 2 Ω at 50 °C to 2.8 Ω at 300 °C.

3. Results and discussion

3.1. Thermal analysis of brake discs and pads

As it is the case in every numerical simulation, the proposed model presents limitations according to the formulated hypotheses. The friction coefficient that is not constant in most of the cases because it is subject to multiple parameters including temperature, exerted pressure, sliding speed … etc. The pressure of contact of the disc pads is not always uniform during the braking process, as well as the material properties that might be modified by the temperature changes. An interpolation has been performed from the available properties at 20 °C and 30 °C in order to determine the air properties at 25 °C for the calculation of the heat transfer coefficient h.

Figs. 5 and 6 show the distribution of 12 temperature ranges throughout brake discs of the full and ventilated types in simulations with the surrounding air temperature set at 25 °C, 0 °C or −20 °C. The highest temperature reached was 222 °C on the surface of the full disc in air at 25 °C (Fig. 5 a.). This maximum dropped by a value approximately equal to each decrease in air temperature (Fig. 5 b. and 5.c.).

These results correspond to fixed conditions in terms of initial speed and component material characteristics.

The relationship between brake temperature and air temperature was conserved in the case of ventilated discs, whereas the

Table 5
Numerical values of the parameters used for the FEM analysis.

Parameter/variable	Value
R_e	$289,623.3$
P_r	0.711
N_u	752.3
h	$68.4 W/m^2 \cdot K$
a	$-4.96 m/s^2$
t_b	$3.4 s$
E_c	$197,996 J$
E_T	$203,936 J$
P	$59,981.2 W$
q_{total}	$996,136.12 W/m^2$
α	0.1
q_{pad}	$996,13.2 W/m^2$

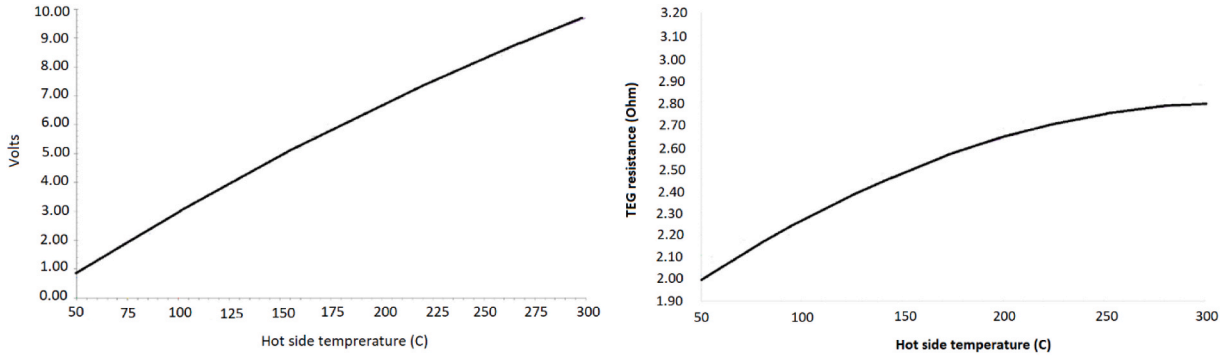

a) Open-circuit output voltage curve. b) Resistance curve

Fig. 4. Open-circuit output voltage and resistance of a TEG as a function of the hot-side temperature: a) Open-circuit output voltage curve, b) Resistance curve (Adapted from Ref. [25]).
a) Open-circuit output voltage curve.
b) Resistance curve

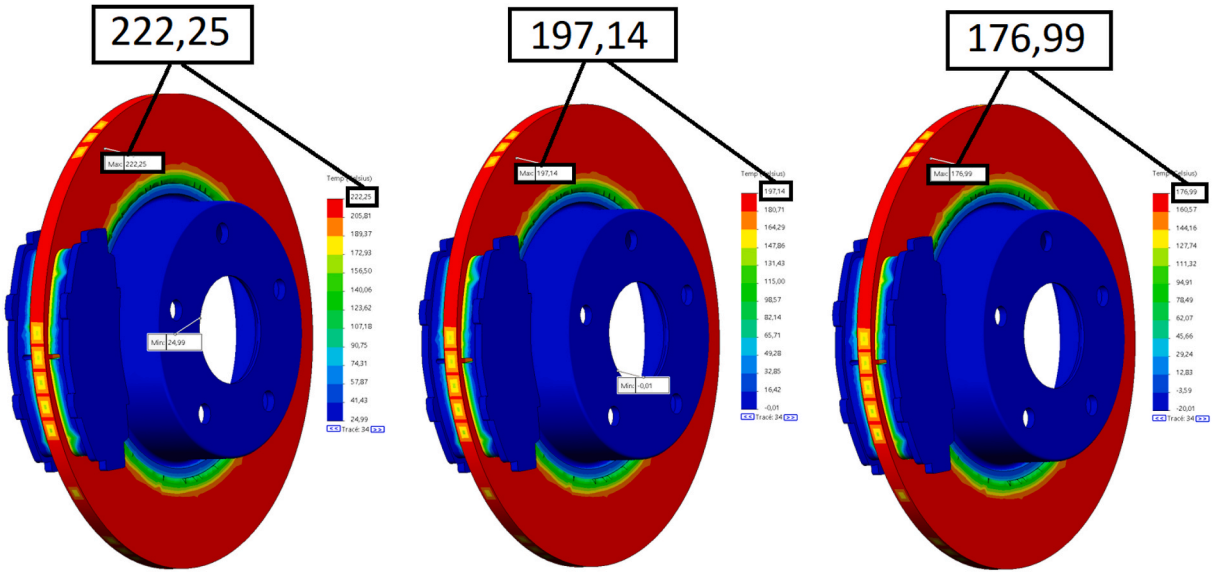

a) Case1: in air at 25°C b) Case2: in air at 0°C c) Case3: in air at -20°C

Fig. 5. Temperature distribution in a full brake disc: a) Case1: in air at 25 °C, b) Case2: in air at 0 °C, c) Case3: in air at −20 °C.
a) Case1: in air at 25°Cb
) Case2: in air at 0°Cc
) Case3: in air at −20 °C

temperatures were lower overall, reaching a maximum of only 175 °C (Fig. 6 a.), since the ventilated design of the disc allows evacuation of thermal energy. Lower ambient temperature helps thermal energy loss by increasing ΔT under the same conditions of thermal resistance and convection as it can be observed in Fig. 6 b. and 6.c.

For validation purposes, our results were compared to those obtained in similar FEM based analyses works found in the literature. The results presented in the works were obtained under several conditions including the initial speed, the braking time, the type of the disc: full or ventilated, as well as the ambient temperature and the initial temperature of the disc. Table 6 summarizes the several operating conditions and results.

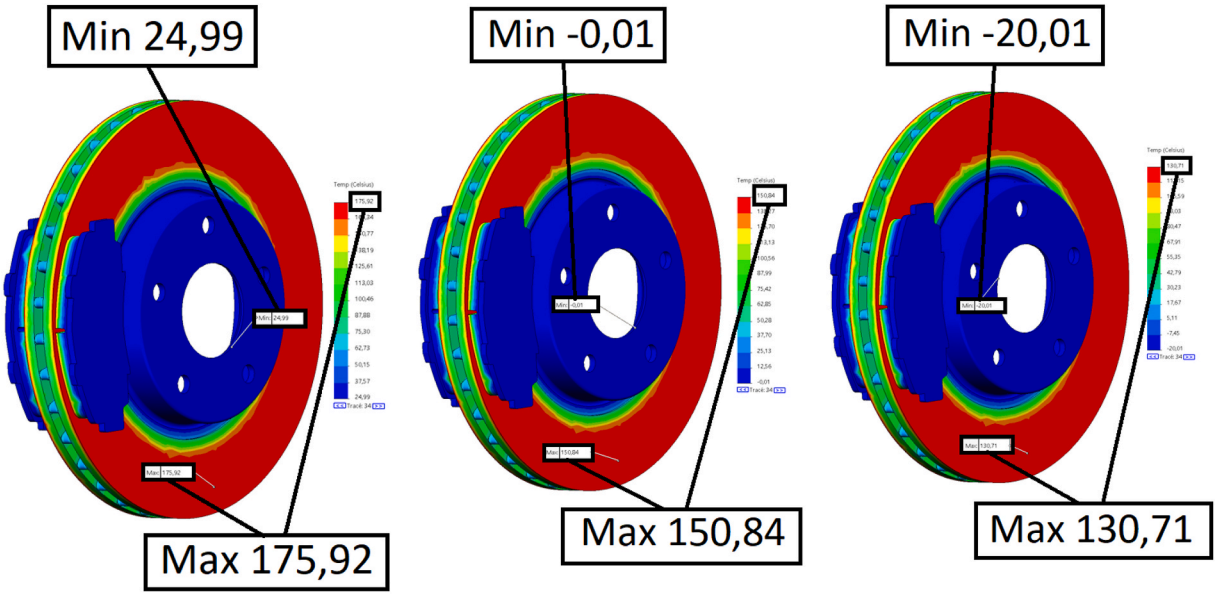

Fig. 6. Temperature throughout a ventilated brake disc: a) Case1: in air at 25 °C, b) Case2: in air at 0 °C, c) Case3: in air at −20 °C.
a) Case 1: in air at 25°Cb
) Case 2: in air at 0°Cc
) Case 3: in air at −20 °C

There are many differences observed in the results from the literature such as the mass of the vehicles, the initial temperature of the disc and some missing data including the ambient temperature and the initial temperature of the disc. Considering these differences, it can be seen from Table 6 that the results presented in this manuscript are within reasonable range of values for the full as well as for the ventilated disc.

The thermoelectric generator delivered 4.25 W when the hot-side temperature of the full disc reached 200 °C and the ambient air temperature was 25 °C. The power generated by the ventilated disc was about 3.25 W or 1 W less than the full disc under the same conditions. Such a result was expected, since the hot-side temperature only reached 175 °C in this case.

One aspect to consider in future work is the availability of the thermal energy, specifically the persistence of the temperature gradient. Belhocine and Bouchetara [2] showed that the temperature reaches a peak value during braking and then drops almost as quickly to a level that drops gradually over a few tens of seconds, as illustrated in Fig. 7 a.

Our experimental curve illustrated in Fig. 7 b. has been obtained using 60 km/h as initial speed, 5 s braking time, with an outside temperature of 20 °C. The curve shows an equivalent behaviour as the one presented in Fig. 7 a.

Due to the limitations of the experimental protocol, the transient phase could not be captured. However, it is apparent that the temperature drops exponentially until it reaches a temperature that remains for more than 10 min and continues to drop very slowly. This emphasises a massive potential of energy recovery during a considerable amount of time after braking. The time available for heat recovery and storage as electrical energy will have major impact on the selection of devices to be used for this purpose.

3.2. Energy conversion

In order to carry out a realistic experiment, we considered temperatures similar to those obtained by FEM analysis. Since the available technical data corresponded to ambient temperatures of 25 °C or higher, performance at 0 °C and −20 °C will be investigated in future work. The portion of the thermal energy presumed to be available during braking will guide the choice of temperatures.

Energy is determined from the open-circuit experiment and the matched load approach, as illustrated in Fig. 8. The matched load approach is performed using a load that is equivalent to the resistance of the TE generator.

A hot-side temperature of 200 °C is considered, based on the results of the thermal analysis of a full disc. The experimental data obtained at an ambient temperature of 25 °C indicate a thermoelectric generator potential $E_{TEG} = 6.5V$, resistance $R_{TEG} = 2.6\ \Omega$, current $I_{TEG} = 1.2A$, output voltage with matched load $V_{TEG} = 3.5V$ and estimated recovered power $P_{TEG} = 4.25W$ or $0.27W/cm^2$. The efficiency is thus about 0.3%, since the recovered energy is 4.25 W while the disc heat flow was estimated at $896,519W/m^2$.

This power is the maximum that can be delivered to a load matching the resistance of the thermoelectric generator. At higher

Table 6
Comparison with the results obtained in the literature.

Reference	Initial speed (Km/h)	Braking time (s)	Wight of the vehicle (Kg)	Ambient temperature (°C)	Initial temperature of the disc (°C)	Full disc temperature(°C)	Ventilated disc temperature(°C)
[2]	28	3.5	1385	–	60	280	240
[7]	80	6	200	–	–	–	173
[8]	90	4	1600	–	–	182	166
[40]	50	4	1800	–	–	226	–
[41]	160	38	–	30	30	–	215
[42]	80	–	1950	–	–	107	–
[43]	100	4	500	–	35	293	169
Our results	60	3.4	1425	25	25	222	176

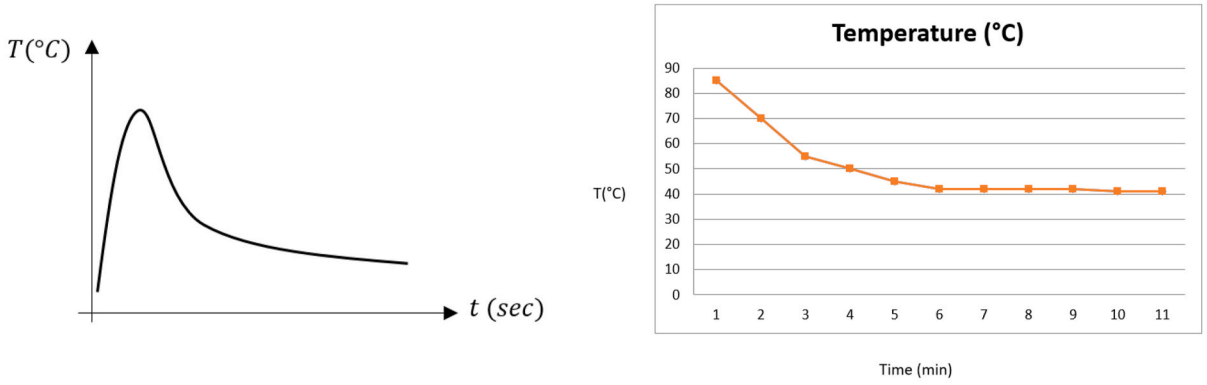

Fig. 7. Post-braking disc temperature curve: a) Typical curve (Image adapted from Ref. [2]), b) Experimental curve.
a) Typical curve (Image adapted from Ref. [2])
b) Experimental curve

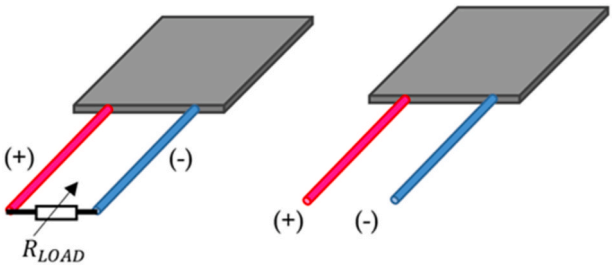

Fig. 8. TEG matched load and open circuit experiment (Image adapted from Ref. [25])

resistances, the power might drop slightly. However, powering on-board devices implies large input impedance values, usually a few mega Ohms. This can be considered to be equivalent to an open-circuit experiment and therefore to involve higher voltages and smaller currents.

4. Conclusions

The use of a thermoelectric generator to recover the thermal energy of automotive braking for conversion into electrical energy to power on-board instrumentation is described. This novel approach to increasing the energy efficiency of motor vehicles is examined by comparing two types of brake discs, namely full and ventilated. Thermal analysis shows that braking produces large rises in the temperature of the disc. Finite elements analysis was conducted for three temperature scenarios including cool and cold climates to calculate the energy available for production of electrical power. The results show that considerable amounts of electrical energy could be recovered, even in cold climates, despite the relatively low efficiency of these thermoelectric devices. At an ambient air temperature of 25 °C, up to 4.25 W were produced in the full-disc brake reaching a hot-side temperature of 200 °C and about 3.25 W or 1 W less in the ventilated disc, which reached a lower hot-side temperature. This confirms that low air temperatures and ventilation of the disc reduce the efficiency of energy recovery by a thermoelectric generator. However, even at efficiencies as low as 0.3%, enough electrical energy could be recovered to power the on-board instrumentation of a typical motor vehicle. Further work is needed on the effects of cold climates on thermoelectric device performance and on brake disc and pad thermal energy flow. The choice of brake materials could have a substantial impact on thermal energy generation and recovery.

Declaration of competing interest

The authors declare that they have no known competing financial interests or personal relationships that could have appeared to influence the work reported in this paper.

References

[1] J.A. Baxter, D.A. Merced, D.J. Costinett, L.M. Tolbert, B. Ozpineci, Review of Electrical Architectures and Power Requirements for Automated Vehicles, IEEE Transportation Electrification Conference and Expo (ITEC), CA, 2018, pp. 944–949, https://doi.org/10.1109/ITEC.2018.8449961.

[2] A. Belhocine, M. Bouchetara, Thermal analysis of a solid brake disc, Appl. Therm. Eng. 32 (1) (2012) 59–67, https://doi.org/10.1016/j.applthermaleng.2011.08.029.

[3] S. Zhou, Z. Guo, X. Bai, Fatigue fracture analysis of brake disc bolts under continuous braking condition, Eng. Fail. Anal. 115 (1) (2020) 104588, https://doi.org/10.1016/j.engfailanal.2020.104588.

[4] P. Grzes, Finite element analysis of disc temperature during braking process, Acta Mech. Automatica 3 (4) (2009) 36–42.

[5] S. Satope, M. Bote, S.D. Rawool, Thermal analysis of disc brake, International Journal for Innovative Research in Science & Technology 3 (2017).

[6] A. Belhocine, C.D. Cho, M. Nouby, Y.B. Yi, A. Abubakar, Thermal analysis of both ventilated and full disc brake rotors with frictional heat generation, Applied and Computational Mechanics 8 (1) (2014) 5–24.

[7] A.N. Phaneendra, S.J. Razi, W.U. Kareeml, G.M. Adnan, S.M. Abdulahad, Thermal analysis of solid disc brake rotor, Int. J. Mech. Prod. Eng. Res. Dev. 8 (12) (2018) 1039–1048.

[8] S. Mačužić, I. Saveljić, J. Lukić, J. Glišović, N. Filipović, Thermal analysis of solid and vented disc brake during the braking process, Journal of the Serbian Society for Computational Mechanics 9 (12) (2015) 19–26.

[9] Y.V.N. Chandana, K.V.P. Reddy, Transient thermal analysis of AlSiCp composite disc brake, Int. J. Comput. Eng. Res. 7 (12) (2017) 2250–3005.

[10] Q. Jian, L. Wang, Y. Shu, Thermal analysis of ventilated brake disc based on heat transfer enhancement of heat pipe, Int. J. Therm. Sci. 155 (2020) article 106356.

[11] Q. Jian, Y. Shui, Numerical and experimental analysis of transient temperature field of ventilated disc brake under the condition of hard braking, Int. J. Therm. Sci. 122 (1) (2017) 115–123.

[12] T.V. Manjunath, P.M. Suresh, Structural and thermal analysis of rotor disc of disc brake, International Journal of Innovative Research in Science, Engineering and Technology 2 (12) (2013) 7741–7749.

[13] P. Grzes, Maximum temperature of the disc during repeated braking applications, Adv. Mech. Eng. 11 (3) (2019) 1–13, https://doi.org/10.1177/1687814019837826.

[14] F.M.D. Zabek, Solid state generators and energy harvesters for waste heat recovery and thermal energy harvesting, Thermal Science and Engineering Progress 9 (1) (2019), 235-24.

[15] S. Sarkar, P.P. Rathod, Review paper on thermal analysis of ventilated disc brake by varying design parameters, Int. J. Eng. Res. Technol. 2 (12) (2013).

[16] D. Champier, Thermoelectric generators: a review of applications, Energy Convers. Manag. 140 (1) (2017) 167–181.

[17] H. Tian, N. Jiang, Q. Jia, X. Sun, G. Shu, X. Liang, Comparison of segmented and traditional thermoelectric generator for waste heat recovery of diesel engine, Energy Procedia 75 (1) (2015) 590–596.

[18] N. Salamon, Development of Thermal Energy Harvesting Systems. Doctoral Thesis, Grenoble University Alpes, 2018.

[19] A. Porto, D. Bibbo, M. Cerny, D. Vala, V. Kasik, L. Peter, S. Conforto, M. Schmid, M. Penhaker, Thermal energy harvesting on the bodily surfaces of arms and legs through a wearable thermo-electric generator, Sensors 18 (6) (2018) 1927, https://doi.org/10.3390/s18061927.

[20] S. Maharaj, Design and Implementation of a Thermoelectric Cogeneration Unit. Master Thesis, Durban University of Technology, 2016.

[21] A. Tahami, M. Gholiakhani, S. Dessouky, A. Montoya, A.T. Papagiannakis, L. Fuentes, L.F. Walubita, Evaluation of a roadway thermoelectric energy harvester through FE analysis and laboratory tests. International Journal of Sustainable Engineering, Taylor & Francis (2021) 1–17.

[22] RMT, Thermoelectric Power Generating Solutions, 1MD02-035-xxTEG Datasheet, 2018.

[23] T.E.C. Specifications, TEG Module TEG1-12611-6.0, TEC Solid-State Power Generators, 2014. https://thermoelectric-generator.com/wp-content/uploads/2014/04/SpecTEG1-12611-8.0Thermoelectric-generator.pdf.

[24] J. Wu, A Basic Guide to Thermocouple Measurements. Application Report, Texas Instruments, 2018.

[25] TEC, Specifications TEG Module TEG2-07025HT-SS, TEC Solid state power generators. https://tecteg.com/wp-content/uploads/2014/09/Spec-TEG2-07025HT-SS-rev1-1.pdf, 2014.

[26] T.E.C. Thermoelectric, TEG specification sheet. https://customthermoelectric.com/media/wysiwyg/TEG_spec_sheets/1261G-7L31-04CQ_20140514_spec_sht.pdf, 2014.

[27] EG-DMO, Hand heat thermoelectric generator (TEG) demonstrator. datasheet, rev 1.1. https://txlgroup.com/wp-content/uploads/2018/06/TEG-DMO-data-sheet-rev-1-1.pdf, 2018.

[28] Tempsens. Type K thermocouple. https://api.ferguson.com/dar-step-service/Query?ASSET_ID=5044326&USE_TYPE=SPECIFICATION&PRODUCT_ID=531968.

[29] T.Y. Kim, J. Kwak, B.W. Kim, Energy harvesting performance of hexagonal shaped thermoelectric generator for passenger vehicle applications: an experimental approach, Energy Convers. Manag. 160 (1) (2018) 14–21.

[30] M.A. Zoui, S. Bentouba, J.G. Stocholm, M. Bourouis, A review on thermoelectric generators: progress and applications, Energies 13 (14) (2020), 3606, 2020.

[31] D. Kim, C. Kim, J. Park, T.Y. Kim, Highly enhanced thermoelectric energy harvesting from a high-temperature heat source by boosting thermal interface conduction, Energy Convers. Manag. 183 (1) (2019) 360–368.

[32] Honda proclame sa Civic voiture la plus vendue au Canada (encore) en 2017, News Paper, La presse, 04 01 2018, in: https://www.lapresse.ca/auto/actualites/honda/201801/04/01-5148989-honda-proclame-sa-civic-voiture-la-plus-vendue-au-canada-encore-en-2017.php. (Accessed 13 September 2020).

[33] B. Charrette, Honda, Civic 2018: La plus populaire. L'annuel de l'automobile, 15 03 2018. https://www.benoitcharette.com/honda-civic-2018-plus-populaire/. (Accessed 13 September 2020). Accessed.

[34] Solidworks (27.3.0.00.52. www.solidworks.com/fr, 2019-2020.

[35] M. Araiz, D. Astrain, A. Martínez, Thermoelectric generators for waste heat harvesting: a computational and experimental approach, Energy Convers. Manag. 148 (1) (2017) 680–691.

[36] J.L. Meriam, L.G. Kraige, Engineering Mechanics: Dynamics, seventh ed., Book, Virginia Polytechnic Institute and State University, John Wiley & Sons Inc, 2012.

[37] H. Lü, D. Yu, Brake squeal reduction of vehicle disc brake system with interval parameters by uncertain optimization, J. Sound Vib. 333 (26) (2014) 7313–7325.

[38] Tableau 1, Propriétés thermiques de différents produits solides non alimentaires (Holman, 1990; Bimbenet et al), Available on line, https://docplayer.fr/10506903-Tableau-1-proprietes-thermiques-de-differents-produits-solides-non-alimentaires-holman-1990-bimbenet-et-al.html. (Accessed 13 September 2020).

[39] D. Luo, R. Wang, W. Yu, W. Zhou, A novel optimization method for thermoelectric module used in waste heat recovery, Energy Convers. Manag. (2020) 209, article 112645.

[40] Y. Tabbai, A. Alaoui-Belghiti, R. El Moznine, F. Belhora, A. Hajjaji, A. El Ballouti, Friction and wear performance of disc brake pads and pyroelectric energy harvesting, International Journal of Precision Engineering and Manufacturing-Green Technology 8 (2021) (2020) 487–500.

[41] V. Sai Naga Kishore, K.P. Vineesh, Temperature evolution in disc brakes during braking of train using finite element analysis, Materials Today, Proceedings 41 (2021) (2020) 1078–1081.

[42] R.A. García-León, et al., Thermo-mechanical assessment in three autoventilated disc brake by implementing finite elements, J. Phys. Conf. (2019).

[43] J. Jamari Jaenudin, M. Tauviqirrahman, Thermal analysis of disc brakes using finite element method, International Conference on Engineering, Science and Nanotechnology (2016).